Note: Vertical distribution of Chl in Lake Leman and impact on measurable radiance (or reflectance)

Contents

From (Baracchini et al., 2020): Observations of the true system also require quantifying their uncertainties, as measurements are always an imperfect and incomplete representation (Bertino et al., 2007). This is particularly important as it defines how reliable an observation is and therefore how the model states are corrected. Injecting data with incorrect measurement error distributions into a good model could depreciate its relevance to the point at which assimilation estimates are worse than the non-assimilative solution or the observations. The opposite holds true, and model forecast would still be unreliable.

vertical non-uniformities are a major obstacle to provide accurate remote sensing products in oligo to mesotrophic lakes (Nouchi et al., 2018).

Figure 1. Image Sentinel 2 of Lake Leman (2016-07-24, after atmospheric correction). Red dot shows the location of the permanent sampling station SHL2.

1 Chl vertically intergrated values fro satellite matchup comparisons

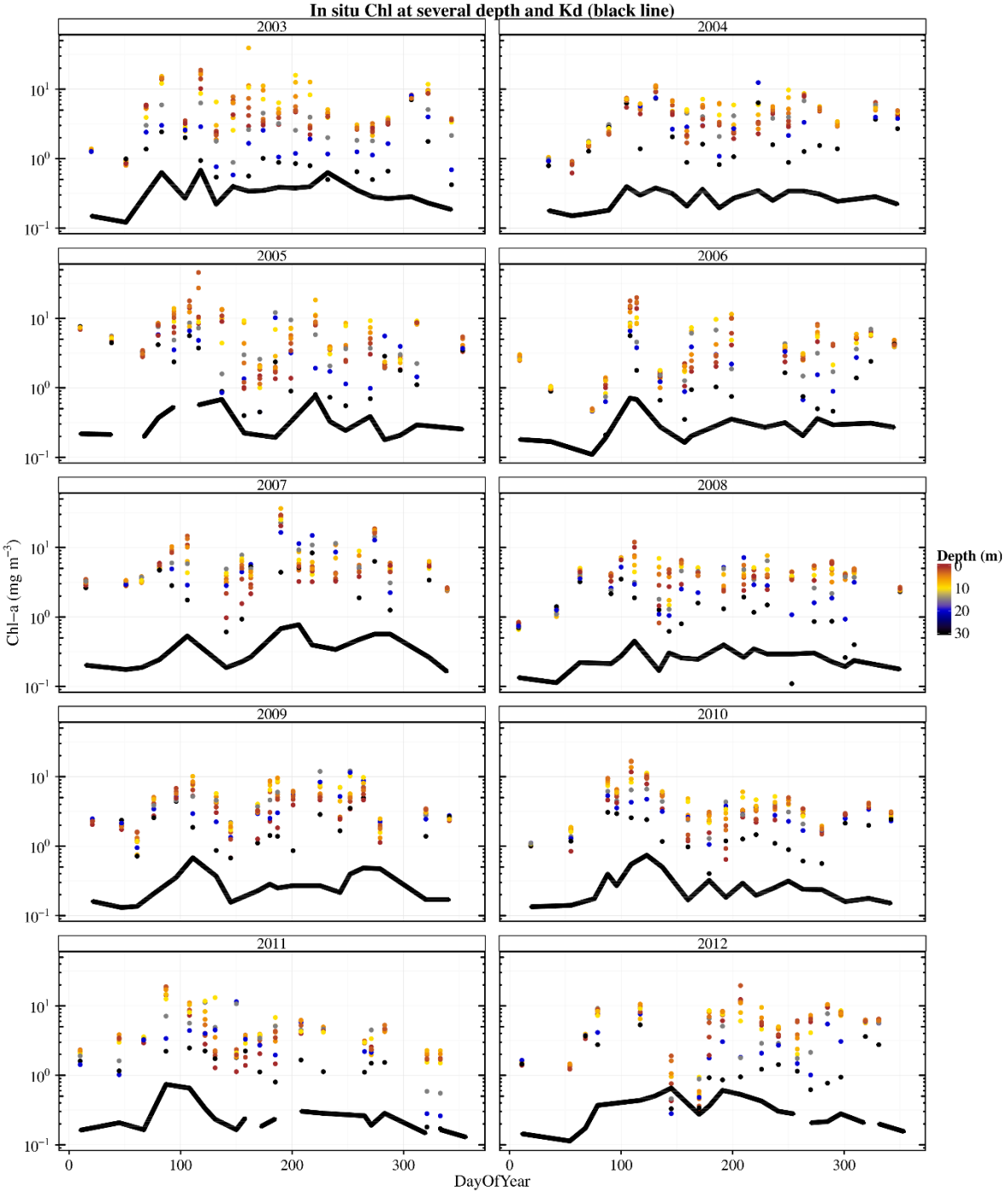

Figure 2. Timeseries of concentration of Chlorophyll-a (Chl-a) measured at the SHL2 station (46.4527N, 6.5887E). The coefficient of diffuse attenuation (K_d, m^{-1}) is calculated from the Secchi Disk depth (SDD) with a basic relationship (i.e., Kd ≡ 1.7 / SDD); see Figure 3.

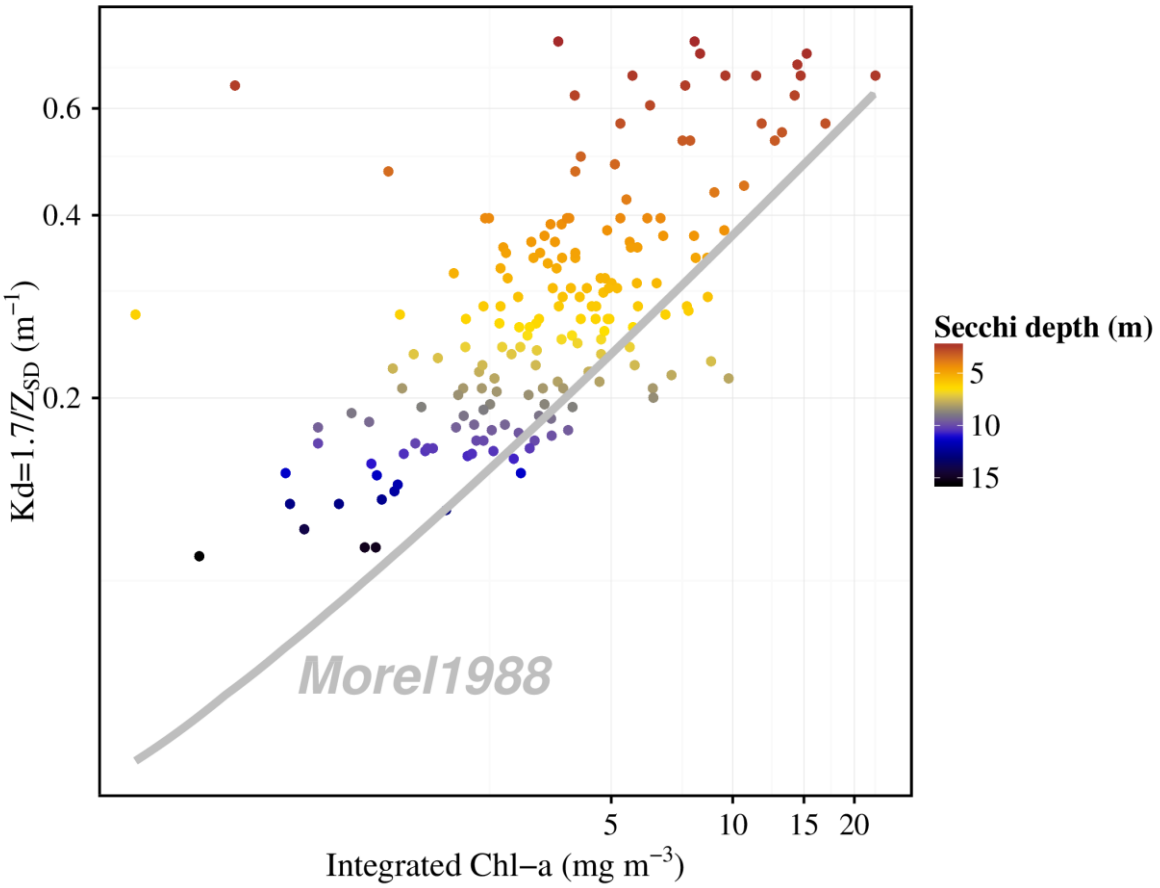

Figure 3. Relation between Kd (calculated from the Secchi disk depth) and the chlorophyll-a concentration weight-averaged over the 30 first meters. This relation departs from that publised by Morel 1988 which was based on open water measurements (Morel, 1988).

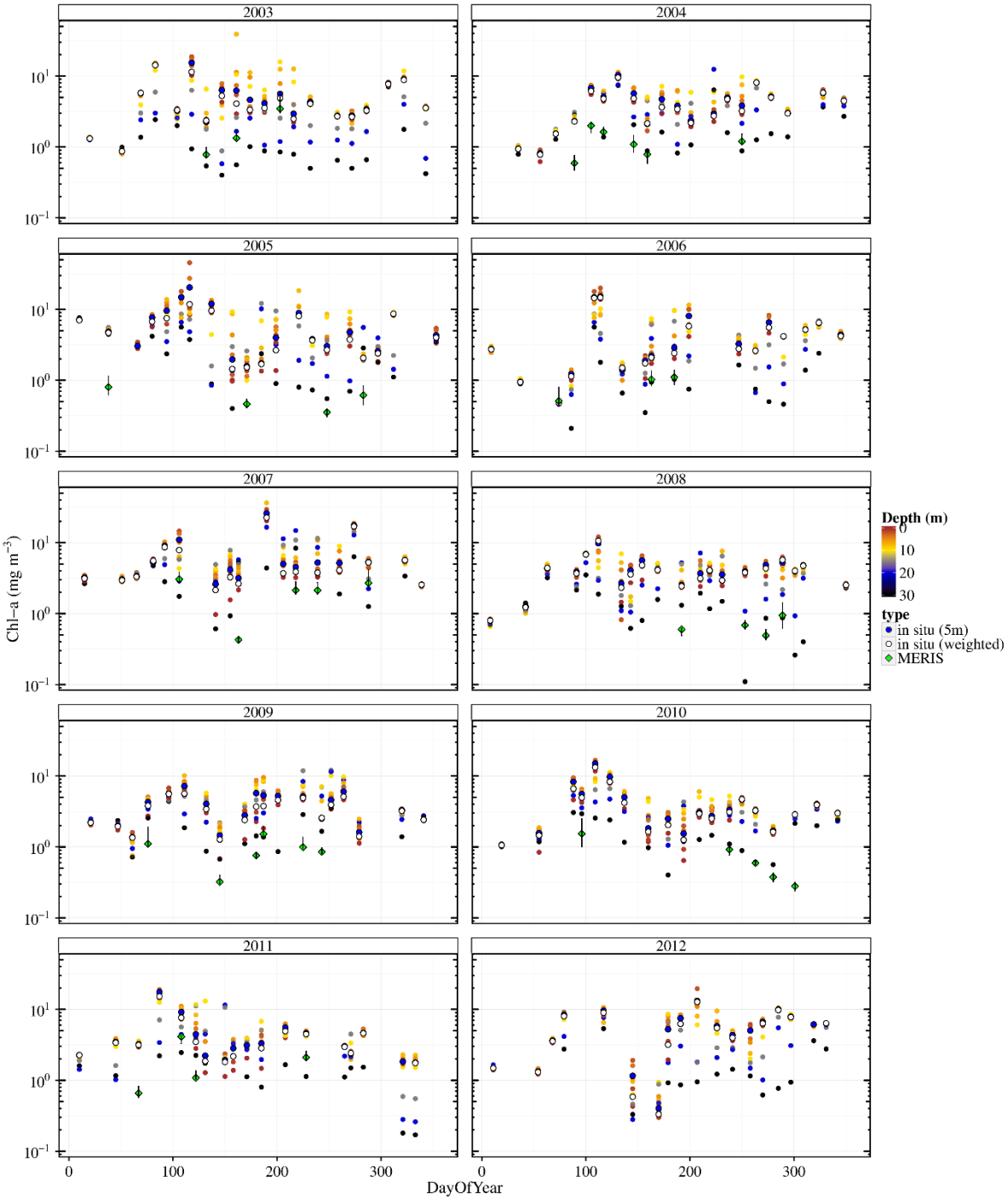

Figure 4. Timeseries of the Chl concentration : measured at several depths (colored dots), taken as the average over the 5 first meters (blue dots) and weighted by the transmittance of the water column to mimic the value actually "sensed" by the satellite device. MERIS retrievals are shonw in green losanges.

$$Chl_{5m} = mean\left(Chl(0 \le depth \le 5m)\right) \quad \textbf{(1)}$$

$$Chl_{weighted} = \frac{\sum_{z=depth} Chl(z)\exp(-2K_d z)}{\sum_{z=depth} \exp(-2K_d z)} \quad \textbf{(2)}$$

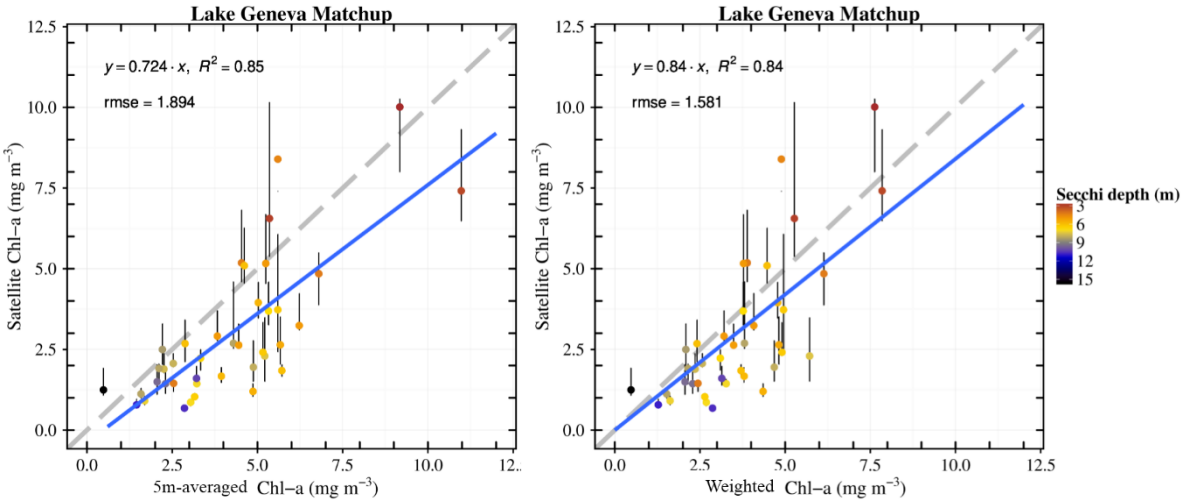

Figure 5. Matchup comparison of MERIS Chl retrievals against reference Chl calculted with the 5 first meters average method (left) and the Kd-weighted method (right). It can be noticed that the second method significantly improved the slope of the regression line and reduced the RMSE between satellite and in situ data.

2 Gaussian modeling of the vertical distribution of Chl

Basic model for Chl vertical distribution (see Figure 6):

$$Chl(z) = B_0 + Chl_{max} \exp\left(-\frac{1}{2}\left(\frac{z - z_{max}}{\sigma}\right)^2\right), \quad \textbf{(3)}$$

with B_0 the background Chl-concentration (constant over depths), z_{max} the depth of the the maximum of Chl, σ the stndard deviation of the normal distribution and Chl_{max} the concentration above background at z_{max}. Such a use of Gaussian formulation permits easy analytical calculation of the vertical-integrated value of Chl_{tot} (i.e., in mg m^{-2}):

$$Chl_{tot}(z_{up}, z_{down}) = B_0(z_{down} - z_{up}) + \frac{Chl_{max}\sigma\sqrt{2\pi}}{2}\left[erf\left(\frac{z_{down} - z_{max}}{\sigma\sqrt{2}}\right) - erf\left(\frac{z_{up} - z_{max}}{\sigma\sqrt{2}}\right)\right] \quad \textbf{(4)}$$

For each measured Chl profile, constrained non-linear optimization was applied to retrieve the four parameters describing the Chl vertical profile (Eq. (3)). Results of the fitting procedure are shown in Figure 7 for the monthly cmiùatology over the 2003-2012 period.

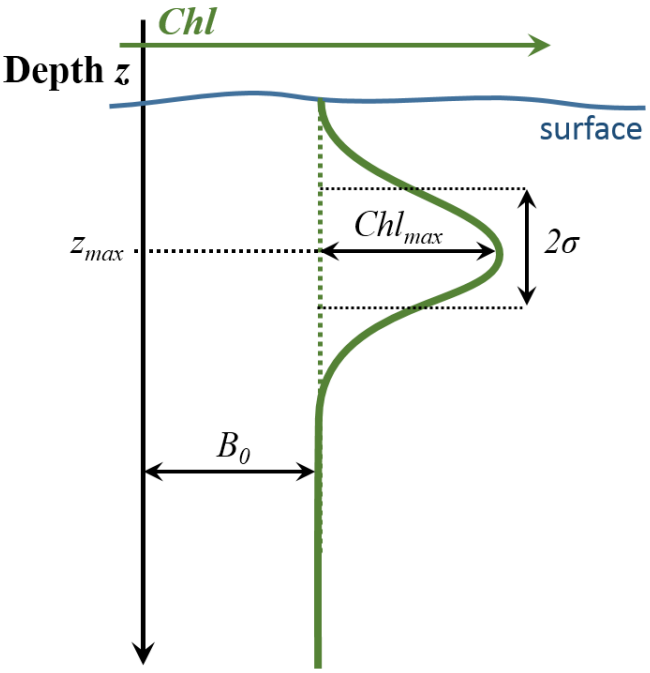

Figure 6. Basic Gaussian model for Chl vertical distribution.

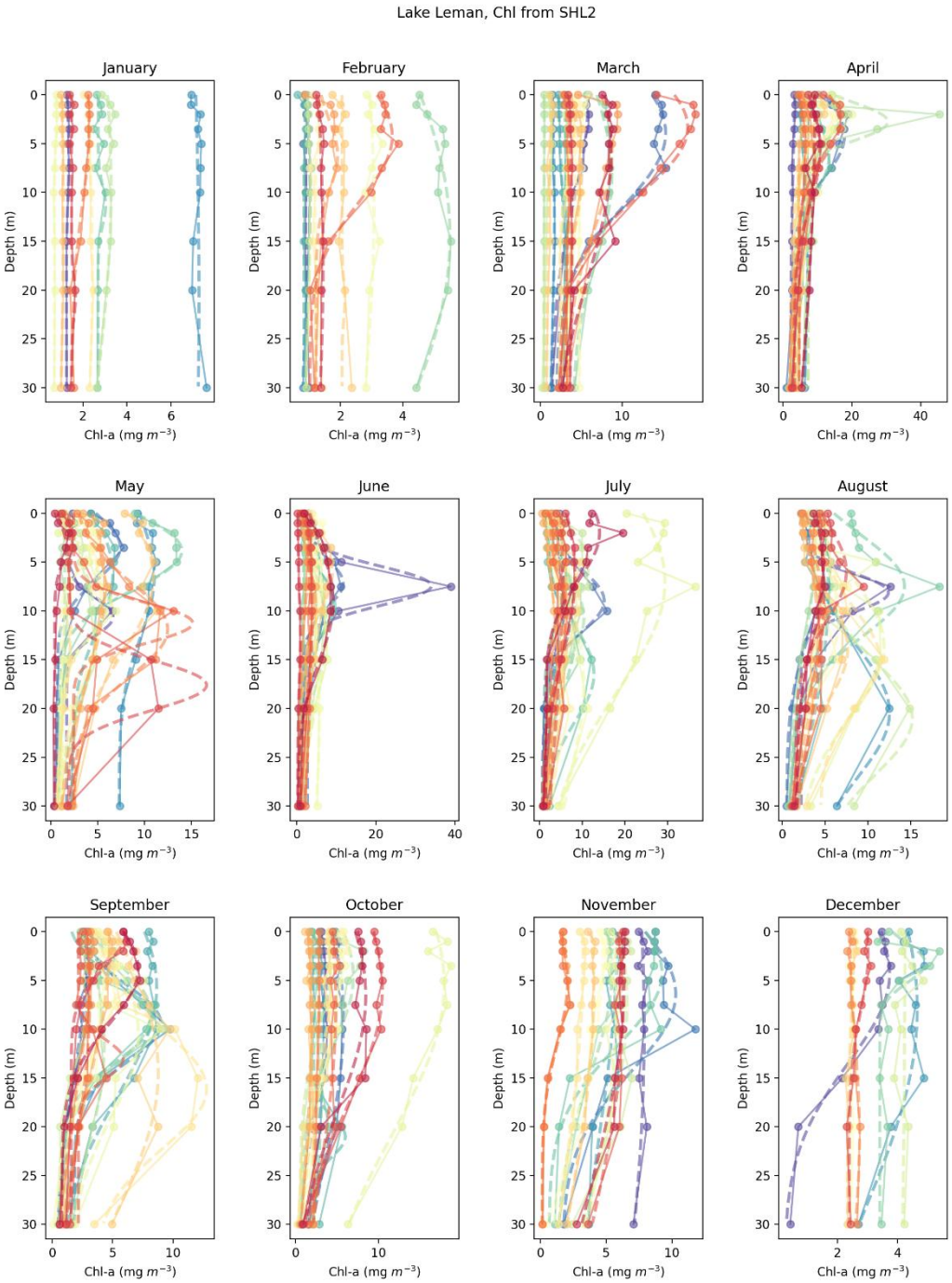

Figure 7. Chl measurements at several depth (colored dots) and corresponding fitted gaussian profiles for data acquired from 2003 to 2012 at SHL2.

Figure 8. Statistics over 2003-2012 showing cross-relations and histograms of the fitted parameters describing the gaussian Chl profiles for the four trimesters (quarters: 1. Jan-Feb-Mar, 2. Apr-May-Jun, 3. Jul-Aug-Sep, 4. Oct-Nov-Dec)

3 Preliminary radiative transfer computations: impacts of vertical profiles on radiances

For a given water-column-integrated Chl_{tot}, several Chl-profiles were used to simulate the water-leaving radiance through radiative transfer computations. The parameters $Chl_{max,}$ σ and z_{max} were prescribed from the typical values obtained in the statistical analysis of Figure 8 as listed in table 1. The paramater B_0 was adjusted based on Eq. (4) for each profile in order to always have the same total chlorophyll Chl_{tot} thus making the simulations comparable. The Chl profiles obtained from table 1 are shown in Figure 9.

Table 1. Parameters used to generate Chl profile for the given value of Chl_{tot} (= 200 mg m^{-2})

#profile	B_0	Chl_{max}	z_{max}	σ
1 (homogeneous)	6.7	0	-	-
2	2.6	15	2	5
3	1.4	15	5	5
4	0.4	15	15	5

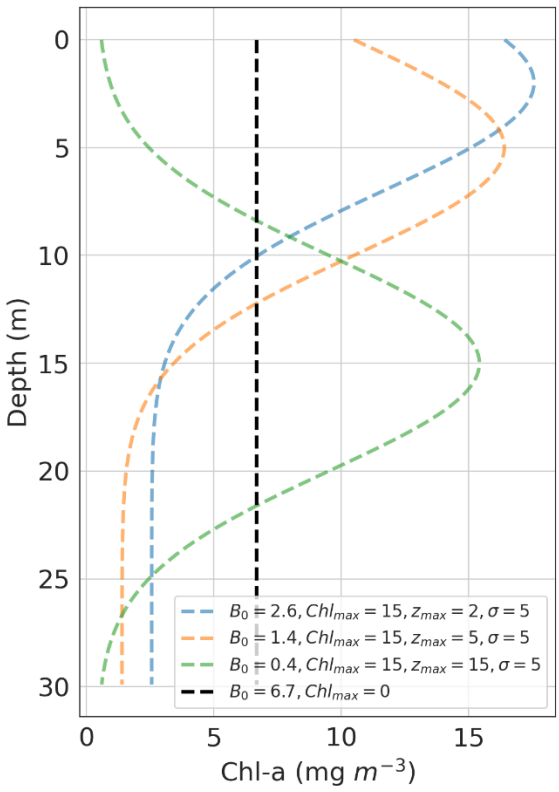

Figure 9. Tabulated synthetic profiles used for radiative transfer computation.

The two following figures show the results of radiative transfer computations performed with the OSOAA code (Chami et al., 2015). It is noticeable that all Stokes parameters and the degree of linear polarization are strongly impacted by the vertical distribution of the phytoplankton in the 30 first meters of the water column Figure 10.

This has critical consequences on the blue/green reflectance ratio (Rrs(440nm)/Rrs(550nm) commonly used for Chl estimation from satellite data (Figure 11).

TODO: figure with Chl estimation from current algorithms.

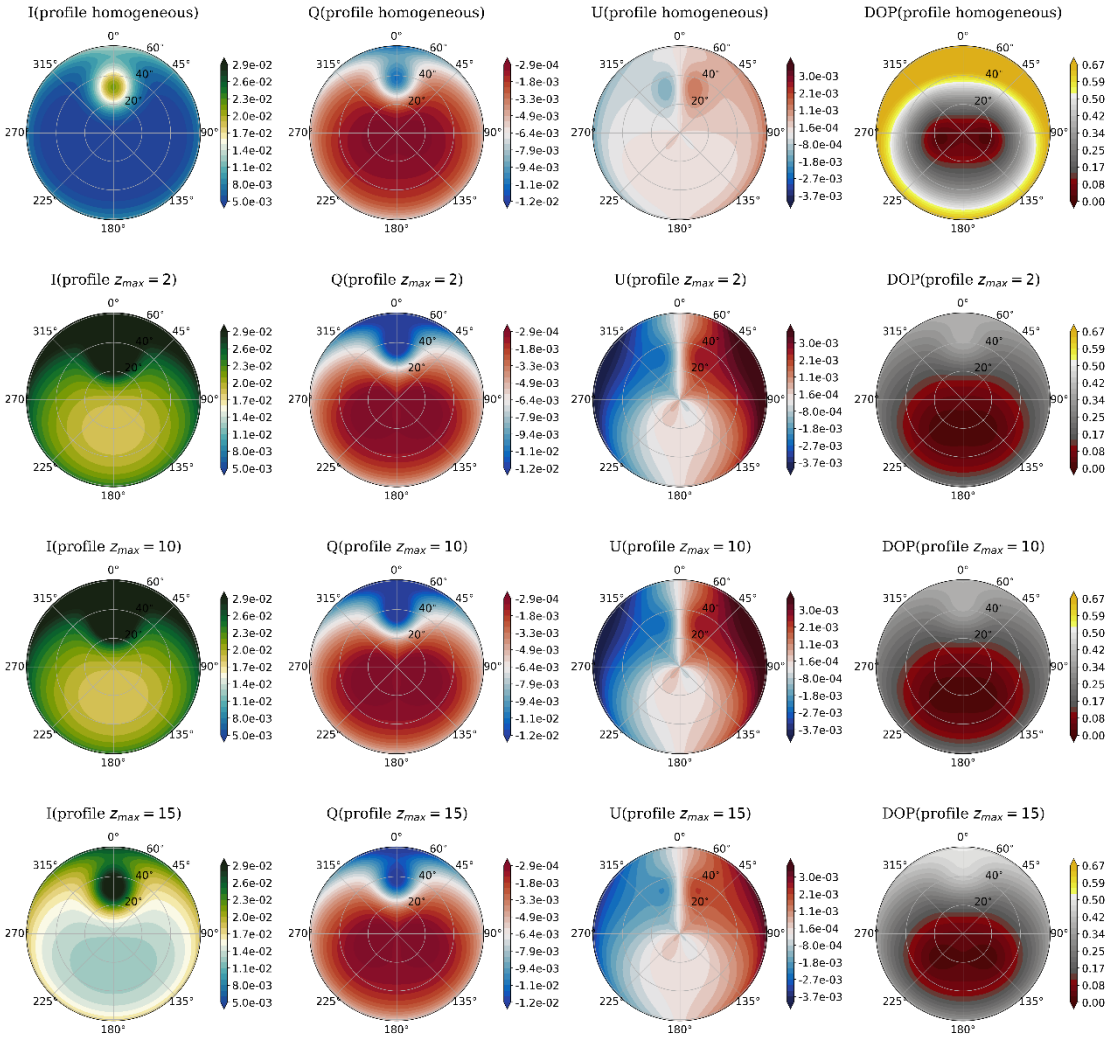

Figure 10. Example of Stokes parameters (I being the normalized radiance) at the lake surface for the different phytoplankton vertical profiles listed in Table 1.

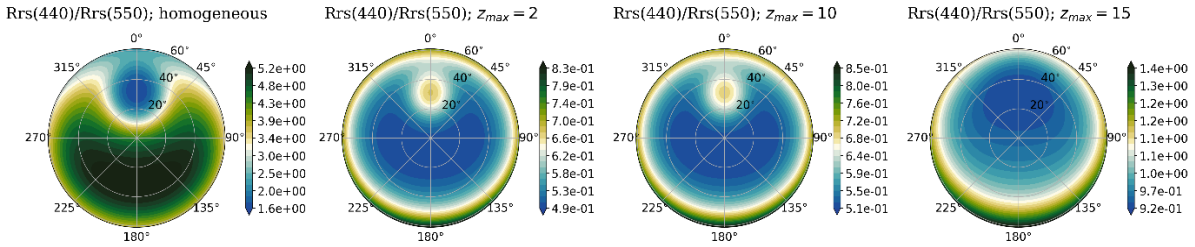

Figure 11. Impact of the vertical distibution on the ratio of Rrs in the blue over the Rrs in the green which is the main component for Chlorophyll-a concentration from MODIS-like satellite mission.

References

Baracchini, T., Chu, P. Y., Šukys, J., Lieberherr, G., Wunderle, S., Wüest, A., & Bouffard, D. (2020). Data assimilation of in situ and satellite remote sensing data to 3D hydrodynamic lake models: a case study using Delft3D-FLOW v4.03 and OpenDA v2.4. *Geoscientific Model Development*, *13*(3), 1267–1284. https://doi.org/10.5194/gmd-13-1267-2020

Bertino, L., Evensen, G., & Wackernagel, H. (2007). Sequential Data Assimilation Techniques in Oceanography. *International Statistical Review*, *71*(2), 223–241. https://doi.org/10.1111/j.1751-5823.2003.tb00194.x

Chami, M., Lafrance, B., Fougnie, B., Chowdhary, J., Harmel, T., & Waquet, F. (2015). OSOAA: a vector radiative transfer model of coupled atmosphere-ocean system for a rough sea surface application to the estimates of the directional variations of the water leaving reflectance to better process multi-angular satellite data over the ocean. *Optics Express*, *23*(21), 27829–27852. https://doi.org/10.1364/OE.23.027829

Morel, A. (1988). Optical modeling of the upper ocean in relation to its biogenous matter content (Case 1 water). *Journal of Geophysical Research*, *93*(C9), 10749–10768.

Nouchi, V., Odermatt, D., Wüest, A., & Bouffard, D. (2018). Effects of non-uniform vertical constituent profiles on remote sensing reflectance of oligo- to mesotrophic lakes. *European Journal of Remote Sensing*, *51*(1), 808–821. https://doi.org/10.1080/22797254.2018.1493360